Journal Homepage: http://ijcpe.uobaghdad.edu.iq
Iraqi Journal of Chemical and Petroleum Engineering
Vol. 26 No. 2 (June 2025) 11 – 21
EISSN: 2618-0707, PISSN: 1997-4884

CO_2 hydrate formation enhancement via bare and hybrid silica nanoparticles effect: Implications for hydrate-based CO_2 sequestration

Sarmad Al-Anssari [a, b, c, *], Dhifaf Sadeq [b, d], Hassanain A. Hassan [a], Ahmed Hamid Al-Taie [d, e], Zain-Ul-Abedin Arian [f]

a Department of Chemical Engineering, College of Engineering, University of Baghdad, Baghdad, Iraq
b Department of Petroleum Engineering, College of Engineering, Al-Naji University, Baghdad, Iraq
c School of Engineering, Edith Cowan University, Joondalup, Australia
d Department of Petroleum Engineering, College of Engineering, University of Baghdad, Baghdad, Iraq
e Gubkin Russian State University of Oil and Gas, Moscow, Russia
f Western Australia School of Mines, Minerals, Energy and Chemical Engineering, Curtin University, 26 Dick Perry Avenue, Kensington 6151, WA, Australia

Abstract

Carbon dioxide geological storage gives tremendous promise for mitigating anthropogenic carbon emissions. CO_2 hydrate has been given rising attention due to its potential in carbon geo-sequestration projects. The effect of silica nanoparticles (SiNPs) on the kinetics of CO_2 hydrate formation was systematically studied at 3.5 MPa and 280 K. Pure (bare) and surface-modified (hybrid) SiNPs were separately characterized and used in this study. The effect of bare and hybrid SiNPs concentrations on the induction time of CO_2 hydrate formation was investigated. A high-pressure, high-temperature stainless steel vessel was used as a hydrate reactor, and pressure-temperature data were continuously recorded to follow the hydrate formation process. Results revealed that the SiNPs significantly impact the kinetics of CO_2 hydrate formation. The increase of Hybrid SiNPs concentration (>0.03 wt% hybrid SiNPs), significantly reduces the induction time and thus accelerates the rapid formation of CO_2 hydrate. In contrast, bare SiNPs showed a lower effect on CO_2 hydrate formation. Further, the increase of bare SiNPs (e.g., >0.07 wt% bare SiNPs) can tend to eliminate the effect of NPs on induction time. Thus, surface-modified SINPs can significantly enhance CO_2 hydrate formation when formulated correctly.

Keywords: CO_2 hydrates; carbon storage; silica nanoparticles; nanofluids; formation kinetics.

Received on 13/04/2025, Received in Revised Form on 21/05/2025, Accepted on 23/05/2025, Published on 30/06/2025

https://doi.org/10.31699/IJCPE.2025.2.2

1- Introduction

Excessive CO_2 emissions and subsequent global warming have become humanity's most emergent challenges. The amount of CO_2 in the air has increased by 30% since the beginning of the Industrial Revolution, reaching a record high of about 414 ppm in the atmosphere [1]. Reducing carbon emissions is an investable requirement for sustainable development, knowing that CO_2 is the main focus for greenhouse gas reduction and control. However, despite the suggested energy alternatives, fossil fuels are still the primary energy source for human activities, which will undoubtedly result in dramatic emissions of CO_2. Carbon capture and storage (CCS) is suggested as an applicable technology for controlling CO_2 in the atmosphere and mitigating climate change [2, 3]. Storing CO_2 in underground geological formations, including saline aquifers [4], depleted hydrocarbon reservoirs [3, 5], deep oceans [6], and mineral carbonization storage [7] has shown promise in reducing emissions to reach the zero net emission target. The long-term geosequestration of CO_2 as hydrate has been a recent research topic for safe and feasible carbon storage applications [8, 9].

Gas hydrates are nonstoichiometric crystalline compounds formed at low temperatures and high pressures by gas (guest) molecules trapped inside a hydrogen-bonded framework of water (cage) molecules. Such hydrates are relevant in a wide range of scientific and industrial applications, including hydrocarbon extraction [10], gas separation [11, 12], gas transportation [13], and carbon dioxide sequestration [8, 14], on which we focus here. The CO_2 hydrate process is an innovative carbon capture and storage (CCS) technology with minimum leak risks, low energy consumption, and low cost. CO_2 hydrate is a crystalline solid where carbon dioxide molecules are trapped inside a lattice of water cages under specific thermodynamic conditions [15, 16].

Technically, CO_2 hydrate is created at relatively slighter thermodynamic situations (e.g., 280 K, 3.5 MPs)

*Corresponding Author: Email: al-anssari@uobaghdad.edu.iq

considering that of hydrogen hydrate (e.g., 275 K, 300 MPa), and nitrogen hydrate (e.g., 279 K, 27.9 MPs), which makes it possible to capture CO_2 from flue gas [17, 18]. Nevertheless, technical challenges, including the long induction time and the slow growth rate of hydrate formation, prevent the practical implementation of the process.

Several studies have been conducted in the last decade to address the thermodynamic and kinetic challenges that limit the application of CO_2 hydrate formations [6, 8, 9]. In this context, it has been found that the addition of suitable chemical promoters can enhance the CO_2 hydrate formation process thermodynamically and kinetically. For instance, thermodynamic promoters, including tetrahydrofuran (THF) [12, 19] and tetrabutylammonium bromide (TBAB) [20], can efficiently reduce the optimum required pressure to initiate hydrate formation process. Moreover, kinetic promoters, including dodecyl trimethylammonium chloride (DTACl) [21], sodium dodecyl benzene sulfonate (SDBS) [22], sodium dodecyl sulfate (SDS) [23], and $_L$-methionine ($_L$-Met) [24] can accelerate hydrate nucleation and growth, leading to higher hydrate formation rate and CO_2 storage capacity. These chemical promoters can be used solely or combined with another promoter type to enhance the gas hydrate process kinetically and thermodynamically. However, using such traditional promoters often suffers from several drawbacks, including the high cost, low efficiency in subsurface conditions with high potential of losing via adsorption at rock surface, foaming tendency, and environmental issues. Thus, innovative additives with unique surface properties are required to enhance the heat and mass transfer of the hydrate formation process.

Recently, nano-materials, including nanoparticles (NPs) and nanofibers, have been extensively studied due to their high surface-to-volume ratio, environment-friendly, tolerance of surface properties, and relatively lower required concentrations for subsurface applications, including tertiary hydrocarbon recovery [25, 26] carbon geosequestration [27], and gas hydrates [28]. Borrowing the idea of Chol [29], who first presented the nanofluids, a suspension of solid NPs in a liquid phase, as new heat transport fluids with higher thermal conductivity, Li, et al. [30] were the first in the literature to suggest the using of nanofluids as kinetic and thermodynamic additives for the gas hydrate initiation process. Their study found that the existence of Cu NPs in the liquid phase significantly shifts the gas hydrate's dissociation pressure and intensifies its kinetic formation. In this context, nanofluids containing metals, metal oxides, or semiconductors have thermal conductivities higher than water by several orders of magnitude, drastically improving gas hydrate nucleation and growth. Several studies investigated the effects of various nanofluids, including dispersions of different NPs in water [7, 11, 18, 31-35], or surfactant solution [22, 36-38] on gas hydrate formations. The reported data of these studies showed that the NPs significantly promote gas hydrate formation by supplying numerous nucleation sites in the liquid phase and strengthening the gas-liquid interface.

In the last decade, silica nanoparticles (SNPs) have also been identified as promoting additives for gas hydrate formation. Ten years ago, Chari, et al. [31] suggested the dispersion of hydrophilic silica nanoparticles (SNPs) in water as a promoter for methane gas hydrate formation in a static reactor. Their results revealed that the yield of methane hydrate was significantly improved in the presence of SNPs, reaching more than 80% when the SNPs to water ratio was adequately optimized. Bai, et al. [39] stated that the hydrophilicity of the SNP surface can transform the local structure of water molecules and gas distribution near liquid-solid interfaces, which alters the mechanism and dynamics of gas hydrate nucleation. Also, their results indicated that hydrate nucleation more effortlessly initiates on comparatively less hydrophilic surfaces. In addition, Nguyen, et al. [40] confirmed that the hydrophobic NPs support the readjustment of liquid molecules to the clathrate H-bond grid assembly, which enhances the hydrate formation process. Kim, et al. [41] probed the crystal structure of CO_2 hydrate with the presence of silica NPs using a scanning electron microscope (SEM). These SEM images suggest the simultaneous generation of CO2 foam and hydrate. Wang, et al. [42] showed that hydrophilic SNPs have a relatively strong inhibition effect on hydrate formation by increasing the induction time by 194% and decreasing the rate of hydrate formation by 10%. Such inhibition effect is mainly related to SNPs' amount, aggregation, and hydrophilicity. Min, et al. [43] conducted a molecular dynamics simulation. They revealed that mono or multi-layer SNPs function as hydrate initiation spots, which move the crystallization initiation of gas to the interface. This contradictory influence of SNPs on the gas hydrate formation process necessitated an extensive investigation of both hydrophilic and hydrophobic SNPs' effect on gas hydrate formation under duplicated working conditions.

This study, thus, investigates the impact of hydrophilic (bare) and hydrophobic (hybrid) SNPs on the kinetics of CO_2 hydrate formation. The studied parameters include hydrate nucleation and induction time. Following our previous work [44], hybrid SNPs were achieved by surface modification of bare SNPs with silane. This approach enables the accurate formulation of nanofluids, which enhances the carbon geo-storage project through an efficient CO_2 hydrate process. The outcomes of this study offer an evaluation approach for hydrate nano-promoters, thus supporting the successive application of hydrate-based CO_2 storage technology.

2- Experimental methods

2.1. Materials

Carbon dioxide (CO_2 gas), with a purity of 99.9 mol%, used in this study was supplied by BOC, gas code-082. Ultrapure deionized (DI) water with a resistivity of 18.25 $m\Omega\, cm^{-1}$, purchased from David Gray, utilized as the base liquid for various nanofluids. Moreover, DI water was also used as a cleaning agent to wash the apparatus before and after each experiment. Further, to prevent

potential contamination, nitrogen gas (purity ≥ 99.9 mol%, from BOC) utilized to dry the equipment after each washing step. Silica (SiO_2) NPs (hydrophilic, 10 – 20 nm, ≥ 99.5 wt%, insoluble, from Sigma-Aldrich) were utilized to formulate various nanofluids and to prepare hydrophilic (hybrid) NPs via the silanization process, which is a reaction of solid particles with silane [44]. 3-aminopropyl triethoxysilane ($H_2N(CH_2)_3Si(OC_2H_5)_3$ Mol wt = 221.37 $g.mol^{-1}$ supplied by Sigma-Aldrich) was used to alter the hydrophilicity of bare SNPs to hydrophobic status. Ethanol (CH_3CH_2OH, purity ≥ 99.5%, ACS reagent, from Sigma-Aldrich) was used as a dispersing medium in the silanization process.

2.2. Alteration of SNPs hydrophilicity via silanization process.

Hydrophilicity is a crucial factor controlling the interfacial behavior of NPs. Typically, the hydrophilicity of NPs can be altered by modifying the surface composition of these solid particles. In this context, a chemical reaction with a silane component is an efficient technique to alter the hydrophilicity of hydrophilic silica surfaces into hydrophobic status [44-48].

The hydrophilicity of SNPs was modified by dispersing 2 g SNPs in 100 mL ethanol and sonicating the mixture using an ultrasonic homogenizer (300 VT, Biologics) with 150 W sonication power for 15 minutes. This relatively low sonication power was used to avoid any unfavorable increase in dispersion temperature due to sonication energy. Simultaneously, a pre-hydrolyzed solution was formulated by adding 1.47 g silane into a mixture of 30 mL ethanol and 0.36 g DI water [44]. The required quantities of 3-aminopropyl triethoxysilane, alcohol, and DI water were based on the number of hydroxyl groups (OH) allocated on 1 g of SNPs. Typically, each 3-aminopropyl triethoxysilane molecule consumes three molecules of DI water for complete hydrolysis [48]. At this stage, the pH of the hydrolysis solution was maintained below the isoelectric point of SNPs, which is around 2, by adding drops of hydrochloric acid. The silane solution was mixed for 30 minutes in a magnetic stirrer and pipetted into the nanodispersion. Subsequently, the obtained mixture was mixed for 24 hours at room temperature to achieve efficient grafting of SNPs with silane. The mixture was then centrifuged, and the silane-treated SNPs were impregnated with an excess amount of ethanol for 48 hours to desorb the reversibly adsorbed silane groups. Ultimately, the silane-treated SNPs were heated at 60 °C for 24 hours to obtain dry hydrophobic (hybrid) SNPs.

2.3. Nanofluid formulation

Nanofluids with different weight concentrations of 0.01, 0.02, and 0.1 wt% bare or hybrid NPs were formulated by adding DI water to 0.002, 0.004, and 0.02 g NPs, respectively, and adjusting the weight of the mixture to 20 g. The ultrasonic homogenizer (300 VT, Biologics) with 150 W sonication power was used for 4 minutes to disperse each sample. Each formulated nanofluid was directly fed to the hydrate apparatus, and the experiment was initiated without delay to minimize the impact of instability on the properties and efficiency of the nanofluid. Furthermore, the particle size distribution and zeta potential of the bare and hybrid SiNPs were measured using dynamic light scattering (DLS) and a zetasizer (ZS), respectively (ZETASIZER Ultra, Malvern Panalytical, UK). The accuracy of such a laser-based technique depends on the transparency of the sample. Thus, dilute samples (e.g., 0.01 wt% SiNPs dispersions) were used for this test [49].

2.4. Characterization of bare and hybrid SiNPs

To understand the crystalline structure of bare and hybrid SiNPs, XRD analysis was conducted using a diffractometer (AERIS, Malvern Panalytical, United Kingdom) with Cu $K_{-\alpha}$ anode at a generator setting of 40 kV and 8 mA, a 2θ range of 10° to 99° at a step size of 0.011° (2θ). Moreover, transmission electron microscopy (TEM, Fortis, nanocomposite, Canada) was used to characterize the morphology, particle size, and cluster size of both bare and hybrid SiNPs, utilizing an electron beam to image the NP sample. Additionally, the Fourier Transform Infrared (FTIR) spectrum was measured using an FTIR spectrometer (PerkinElmer Spectrum 3 FT-IR) to identify and characterize the chemical properties of both bare and hybrid SiNPs.

2.5. Hydrate apparatus

The experimental apparatus is illustrated in Fig. 1, which consists of a high-pressure 0.5-liter stainless steel vessel equipped with a magnetic motor stirrer and an internal cooling coil. A coolant bath with ethylene glycol was used to maintain the system's temperature inside the vessel. The stirrer is used to uniformly distribute the temperature. In this context, hydrate formation mainly depends on the extent of super-cooling, and the hydrate's rapid formation will spontaneously occur near the colder area. Thus, stirring will aid the uniform formation of hydrate. The top cover plate of the vessel had four ports equipped with Swagelok connectors. These ports were used for inserting gas and liquid inlet pipes, the thermocouple, and the pressure transducer. The accuracy of the thermocouple and pressure transducer is ±0.1 K and ±0.08 MPa, respectively. The pressure and temperature signals were collected via data acquisition and sent to the computer. The first high-pressure pump (Teledyne D-500) was used to inject CO_2 and increase the pressure, while the second pump (Teledyne D-260) was used to inject the liquid phase (nanofluid). This pump was also used to vacuum the vessel.

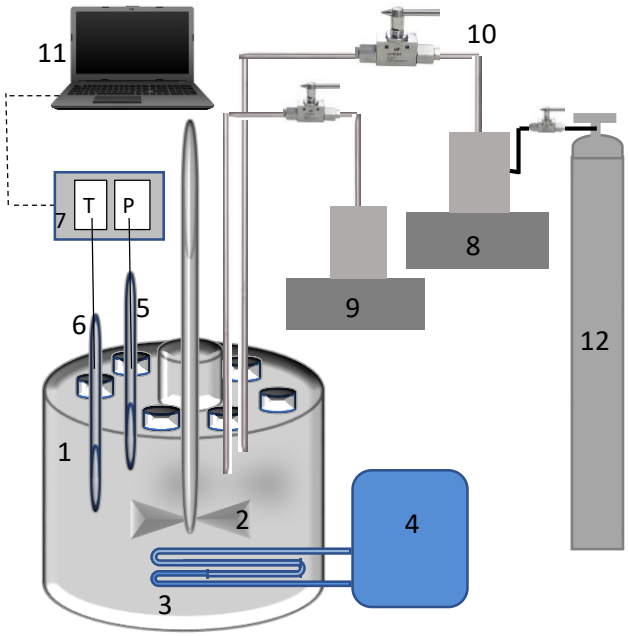

Fig. 1. Detailed schematic diagram of the experimental system: (1) the high-pressure vessel (hydrate reactor), (2) the agitator, (3) the cooling coil, (4) the cooling system, (5) the pressure transducer, (6) the temperature sensor, (7) Data acquisition, (8) CO_2 pump, (9) vacuum and fluids feed pump, (10) valve, (11) data processor, (12) CO_2 cylinder

2.6. Experimental procedure

Before each experiment, the vessel was rinsed with water and dried with nitrogen gas to eliminate any traces or contamination from the air or previous tests. After closing the vessel tightly, the liquid phase (either DI water or a pre-designed nanofluid) was loaded into the high-pressure vessel via a pump. Subsequently, prior to CO_2 injection, the system was vacuumed to remove air, including dissolved air in the liquid phase. Further, CO_2 was fed to the system at a pressure of 0.5 MPa and purged to eliminate any potential remaining air in the vessel. The system's temperature was maintained at a value just above the hydrate temperature of carbon dioxide. The stirrer was switched on to provide a uniform temperature for the system. At this point, carbon dioxide was introduced to the reactor via a high-precision pump to achieve the predesigned pressure. After reaching the set pressure value, the system was allowed to equilibrate for two hours, and the thermodynamic stability of the system was monitored. Accordingly, to start the hydrate formation, the reactor was cooled to a point less than that of equilibrium. The rapid decrease in pressure and the potential gradual increase in temperature are clear signs of gas hydrate formation. The thermodynamic parameters (e.g., P and T) were continuously recorded to investigate the rate of crystal growth and CO_2 consumption. The process is considered completed when no further changes in pressure and temperature are recorded.

3- Results and discussion

3.1. Characterization of bare and hybrid SiNPs

X-ray diffraction (XRD) patterns of bare and hybrid SiNPs are reported in Fig. 2A and Fig. 2B, respectively. XRD results detected a broad peak intense at 2θ = 23°, attributed to the SiNPs, with no other diffraction peaks observed. Reported results confirmed the amorphous nature of both bare and hybrid SiNPs. However, the hybrid SiNPs (Fig. 2B) show comparatively lower noise than the bare SiNPs (Fig. 2A). The reported peak was matched with the reported data in the literature [50].

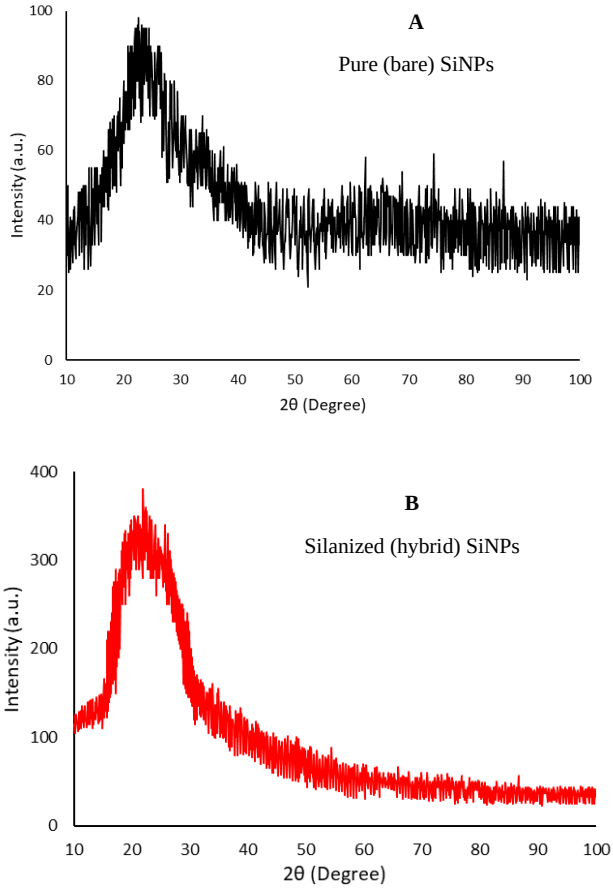

Fig. 2. X-ray diffraction spectra for bare (A) and hybrid (B) SiNPs

The transmission electron microscopy (TEM) images of bare and hybrid SiNPs are shown in Fig. 3 left a Fig. 3 right, respectively. The slight deformation in some parts of the images is related to the device's limitations at such ranges (200 – 300 nm). The particle sizes here are typically less than 100 nm for both SiNPs. The initial size of hybrid SiNPs (Fig. 3 left) is significantly larger than that of bare SiNPs (Fig. 3 right). This is mainly due to the silane groups on the surface of the hybrid SiNPs [47] and the aggregation process during the silanization steps [44].

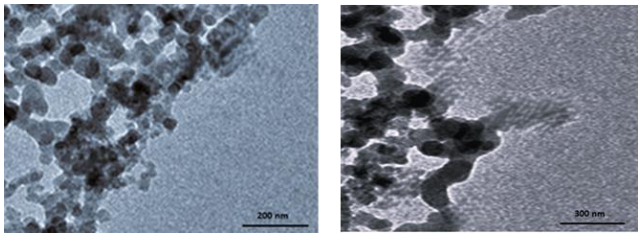

Fig. 3. The TEM images of bare (left) and hybrid (right) SiNPs

The FTIR is shown in Fig. 4 for both bare and hybrid SiNPs. As indicated in Fig. 5, the silane groups have successfully attached to SiNPs, thereby modifying the surface properties of SiNPs. The FTIR spectra of bare and hybrid SiNPs displayed symmetrical vibrations of Si-O-Si at 580 cm^{-1}, Si-O at 800 cm^{-1}, and Si-OH at 975 cm^{-1}. Typically, the absorption band ranging from 850 to 1300 cm^{-1} can be attributed to the overlapping of different SiO_2 peaks and Si-OH peaks and bonds. The strong characteristic absorption band between 3250 and 3450 cm^{-1} can be attributed to O-H, which also appears at 1650 cm^{-1} but with reduced intensity. The differences between the FTIR spectra of bare and hybrid SiNPs are attributed to the adsorption of CH_3, CH_2, and NH_2 groups.

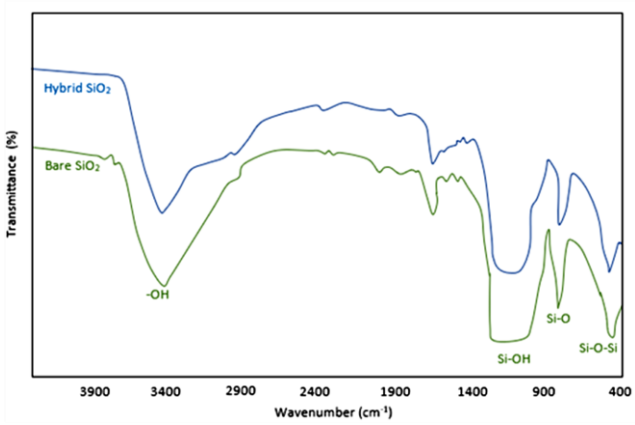

Fig. 4. Comparative FTIR spectra of bare and hybrid SiNPs

3.2. Colloidal properties

The properties of nanofluids, including pH, particle size distribution, and zeta potential of bare and hybrid SiNPs, are presented in Table 1 and Fig. 5 and Fig. 6, respectively.

Table 1. pH of various aqueous phases utilized in the study

The aqueous phase	Conc. of SiNPs	pH
DI water	-	6.25
Bare SiNPs	0.01	6.55
Bare SiNPs	0.05	6.62
Bare SiNPs	0.1	6.65
Hybrid SiNPs	0.01	7.55
Hybrid SiNPs	0.05	7.65
Hybrid SiNPs	0.1	7.75

Table 1 starkly declares that the increase in SiNPs concentration has no significant influence on the pH of the aqueous phase, suggesting that no further action is required to control the pH of the nanofluid by adding drops of HCl or NaOH. Further, the silanization process shifts the pH of SiNPs towards a less acidic range (e.g., pH increases from 6.65 to 7.75), which is consistent with the reported data in the literature [26].

As reported in Fig. 5. Particle size distribution of bare and hybrid SiNPs in the aqueous phase of 0.01 wt% SiNPs at ambient conditions, the average particle size of bare SiNPs was 22 nm with a very narrow particle size distribution. This is mainly due to the direct DLS measurement of the sample after an effective sonication process of the dispersion, which helps avoid undesirable aggregation of NPs. In contrast, hybrid SiNPs exhibit a wide range of particle size distributions with a relatively larger average particle size of around 55 nm, primarily due to the early aggregation of NPs during the silanization step. These numbers are consistent with SEM images of the samples (see Fig. 3).

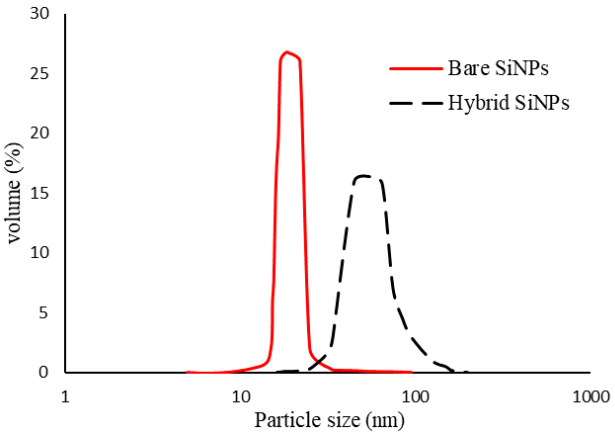

Fig. 5. Particle size distribution of bare and hybrid SiNPs in the aqueous phase of 0.01 wt% SiNPs at ambient conditions

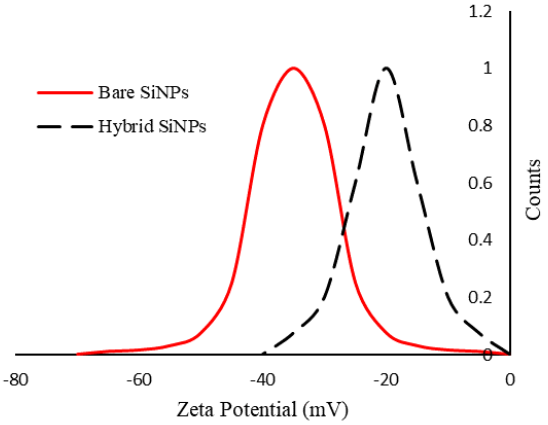

Fig. 6. Zeta potential of bare and hybrid SiNPs in the aqueous phase of 0.01 wt% SiNPs at ambient conditions

The zeta potential of bare and hybrid SiNPs suspensions exhibits negative potentials, indicating a negative charge

on the particle's surface, but with varying extents. Excellent results are demonstrated by bare SiNPs with a zeta potential of approximately -38 mV. Previous studies indicated that nano-dispersions are considered stable when the zeta potential is greater than or equal to ±35 mV [26, 49]. Thus, the bare SiNPs dispersion is within the stable zone. Despite a similar charge, the zeta potential of the hybrid SiNPs displays smaller values of approximately -21 mV, putting such dispersions in the critically stable zone [49]. The zeta potential values can be significantly intensified via mixing with suitable surface-active materials, including anionic surfactants. However, this study was conducted to evaluate the sole effect of various SiNPs on CO_2 hydrate formation without the potential synergistic influence of other additives [51].

3.3. Effect of SiNPs on the Kinetics of CO_2 Hydrate Formation.

Gas dissolution is a crucial factor influencing the formation of gas hydrate. In this context, the nucleation of CO_2 hydrate only starts after reaching a threshold value of CO_2 dissolution in the aqueous phase. [10, 24]. Fig. 7 illustrates the impact of bare and hybrid SiNPs on the dynamics of CO_2 hydrate formation in terms of pressure reduction.

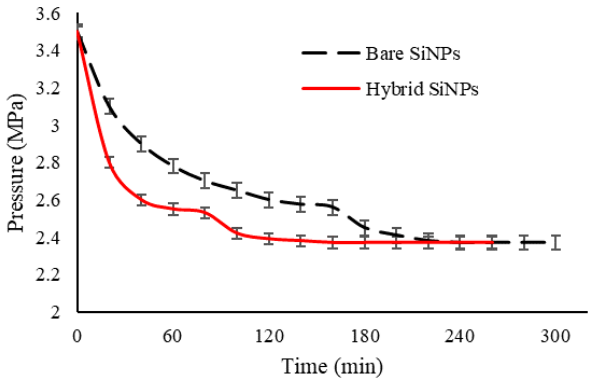

Fig. 7. Pressure reduction over time during CO_2 formation in an aqueous phase of 0.01 wt% SiNPs starting at 3.5 MPa, and 280 K

As detected in Fig. 7, the formation of CO_2 hydrate in aqueous phases of bare or hybrid SiNPs can be separated into three periods, which primarily depend on gas dissolution and hydrate formation. Experimentally, with the presence of bare SiNPs, the pressure in the hydrate reactor was initially reduced from 3.5 to 2.59 MPa within 155 min. At this time, a rapid pressure drop was recorded over a relatively short period from 2.59 to 2.37 within 20 minutes, which was mainly attributed to the consumption of CO_2 inside the reactor. This period is combined, as indicated by the data acquisition unit, with a sharp increase in temperature (not shown in Fig. 7), which relates to the liberation of heat associated with hydrate formation. The total time of these two periods (e.g., 175 min) represents the induction time of hydrate nucleation. In the last period, no further significant reduction of pressure was observed, indicating the end of CO_2 hydrate formation. The stopping of the hydrate formation process is entirely due to pressure reduction, resulting in a low driving force of gas-liquid mass transfer.

In the case of hybrid SiNPs, the three periods of hydrate formation were also observed. However, the induction time of hydrate nucleation was significantly shorter (around 42%) than that of bare silica. This is potentially due to the higher dissolution rate of CO_2 in the liquid phase, which is crucial for the formation of hydrate. Typically, hybrid SiNPs modified with silane groups are oil-wet particles [45]. Al-Anssari, et al. [27] have revealed that the oil-wet surface is CO_2-wet. Thus, mechanistically, CO_2 species at the CO_2/aqueous phase interface attach to the oil-wet hybrid SiNPs and travel to the bulk of the aqueous phase due to the continuous Brownian motion of NPs in the dispersion. Subsequently, hybrid SiNPs act as carriers to enhance the solubility and mobility of CO_2 gas in the liquid phase, thus accelerating the nucleation period. It was not possible to compare with hydrate formation in DI water since no hydrate is possible to form under such conditions with DI water.

3.4. Effect of SiNPs on the induction time

The influences of different concentrations of bare and hybrid SiNPs on the induction time for CO_2 hydrate formations under 3.5 MPa and 280 K are presented in Fig. 8.

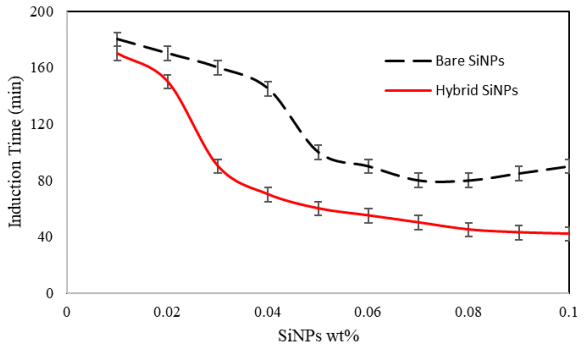

Fig. 8. Effect of SiNPs wt% on the induction time of CO2 hydrate formation at 3.5 MPs and 280 K

Results obviously declare that SiNPs significantly reduce the induction time of CO_2 hydrate formation, and hybrid SiNPs showed a more significant impact on conduction time reduction with lower concentrations (e.g., 0.03 wt% hybrid SiNPs). This is mainly due to the high activity of hybrid SiNPs as transport agents of CO_2 species from the gas/aqueous phase interface to the CO_2 hydrate zone inside the aqueous phase. While the relatively longer induction time with the presence of bare SiNPs, compared to the hybrid one, is typically related to the hydrophilic nature of the bare silica surface that keeps the nanoparticles trapped in the bulk of the liquid phase away from the CO_2/aqueous phase interface [52, 53]. Such a phenomenon reduces the potential for CO_2 carriers to act from the interface to the hydrate zone in the liquid

phase [54]. Mechanistically, despite the Brownian motion of NPs, only a limited number of bare SiNPs can reach the interface, and this number typically increases with concentration (e.g., 0.04 < bare SiNPs wt% < 0.07). A further increase in bare SiNPs concentration (e.g., > 0.7 wt%) can surprisingly increase the induction time. This is potentially due to the aggregation of bare SiNPs at higher concentrations, resulting from the increased number of particles per unit area and thus increased collisions and coalescence precursors of NPs.

4- Conclusion

In this work, the influence of bare (pure) and hybrid (silanized) silica nanoparticles (SiNPs) on the formation kinetics of CO_2 hydrate was systematically investigated. Hybrid SiNPs were produced via silanizing SiO_2 NPs with 3-aminopropyl triethoxysilane. Results reported that an increase in the load of NPs enhances the rapid uptake rate and reduces the hydrate formation time. However, excessively high concentrations of bare SiNPs can hinder hydrate growth.

By adding SiNPs, the nucleation induction time is significantly reduced by a significant period. This is potentially due to the high surface energy and Brownian motion of NPs in the liquid phase, which boosts gas-liquid mass transfer between the interface and bulk of the liquid, thereby facilitating the effective nucleation of CO_2 hydrate. Mechanistically, the extremely small size of SiNPs enables them to carry CO_2 species and travel from the CO_2/aqueous phase interface and travel within the capillary pore channels of the simultaneously formed CO_2 hydrate, thereby facilitating the continuous growth of the hydrate. Furthermore, the presence of SiNPs effectively enhances the rapid diffusion of generated heat during hydrate formation, ensuring rapid and efficient CO_2 storage. In this context, despite the smaller initial size of bare SiNPs, hybrid SiNPs were more efficient in enhancing the hydrate nucleation and growth process. This is mainly due to the instability of bare SiNPs and the rapid aggregation of such pure nano-species. Thus, unlike CO_2 hydrate formation experiments with only pure water, utilizing SiNPs and particularly hybrid NPs improves CO_2 uptake and decreases the induction time.

References

[1] L. Zhang, Q. Zhou, Z. Wang, and W. Lu, "Experimental study on the flux-controlled growth of CO2-SO2 hydrates: Implications for hydrate-based CO2 sequestration," *Chemical Engineering Science*, vol. 298, p. 120369, 2024/10/05/ 2024. https://doi.org/10.1016/j.ces.2024.120369

[2] S. Iglauer, M. S. Mathew, and F. Bresme, "Molecular dynamics computations of brine–CO2 interfacial tensions and brine–CO2–quartz contact angles and their effects on structural and residual trapping mechanisms in carbon geo-sequestration," *Journal of Colloid and Interface Science*, vol. 386, no. 1, pp. 405-414, 11/15/ 2012. http://dx.doi.org/10.1016/j.jcis.2012.06.052

[3] S. F. J. Al-Anssari, "Application of Nanotechnology in Chemical Enhanced Oil Recovery and Carbon Storage," Curtin University, 2018.

[4] P. K. Bikkina, "Contact angle measurements of CO2–water–quartz/calcite systems in the perspective of carbon sequestration," *International Journal of Greenhouse Gas Control*, vol. 5, no. 5, pp. 1259-1271, 9// 2011. http://dx.doi.org/10.1016/j.ijggc.2011.07.001

[5] N. Kumar *et al.*, "Carbon capture and sequestration technology for environmental remediation: A CO2 utilization approach through EOR," *Geoenergy Science and Engineering*, vol. 234, p. 212619, 2024/03/01/ 2024. https://doi.org/10.1016/j.geoen.2023.212619

[6] Q. Sun and Y. T. Kang, "Review on CO2 hydrate formation/dissociation and its cold energy application," *Renewable and Sustainable Energy Reviews*, vol. 62, pp. 478-494, 2016/09/01/ 2016. https://doi.org/10.1016/j.rser.2016.04.062

[7] J. J. Ramsden, I. J. Sokolov, and D. J. Malik, "Questioning the catalytic effect of Ni nanoparticles on CO2 hydration and the very need of such catalysis for CO2 capture by mineralization from aqueous solution," *Chemical Engineering Science*, vol. 175, pp. 162-167, 2018/01/16/ 2018. https://doi.org/10.1016/j.ces.2017.09.042

[8] M. Aminnaji *et al.*, "CO2 Gas hydrate for carbon capture and storage applications – Part 1," *Energy*, vol. 300, p. 131579, 2024/08/01/ 2024. https://doi.org/10.1016/j.energy.2024.131579

[9] M. Aminnaji *et al.*, "CO2 gas hydrate for carbon capture and storage applications – Part 2," *Energy*, vol. 300, p. 131580, 2024/08/01/ 2024. https://doi.org/10.1016/j.energy.2024.131580

[10] M. R. Walsh, C. A. Koh, E. D. Sloan, A. K. Sum, and D. T. Wu, "Microsecond simulations of spontaneous methane hydrate nucleation and growth," *Science*, vol. 326, no. 5956, pp. 1095-1098, 2009. https://doi.org/10.1126/science.1174010

[11] N. Adibi, M. Mohammadi, M. R. Ehsani, and E. Khanmohammadian, "Experimental investigation of using combined CH4/CO2 replacement and thermal stimulation methods for methane production from gas hydrate in the presence of SiO2 and ZnO nanoparticles," *Journal of Natural Gas Science and Engineering*, vol. 84, p. 103690, 2020/12/01/ 2020. https://doi.org/10.1016/j.jngse.2020.103690

[12] M. S. Sergeeva, A. N. Petukhov, D. N. Shablykin, N. A. Mokhnachev, I. V. Vorotyntsev, and V. M. Vorotyntsev, "INVESTIGATION OF THE GAS HYDRATE EQUILIBRIUM IN CH4 - CO2 - H2O MIXTURE IN THE PRESENCE OF THF - SDS PROMOTERS," *Fluid Phase Equilibria*, vol. 546, p. 113170, 2021/10/15/ 2021. https://doi.org/10.1016/j.fluid.2021.113170

[13] Y. Al-okbi, S. Al-Anssari, A. S. N. Al-murshedi, S. K. M. Ibrahim, and R. Al-Dujele, "Simulation and experimentation study on the performance of metal hydride storage vessels," *International Journal of Energy Research*, vol. 46, no. 4, pp. 4187-4203, 2022. https://doi.org/10.1002/er.7420

[14] X. Zhang, M. Zhang, P. Li, J. Li, Y. Wang, and Q. Wu, "Cooperative effect of surfactant and porous media on CO2 hydrate formation and capacity of gas storage," *Fuel*, vol. 329, p. 125494, 2022/12/01/ 2022. https://doi.org/10.1016/j.fuel.2022.125494

[15] S. Sinehbaghizadeh, A. Saptoro, and A. H. Mohammadi, "CO2 hydrate properties and applications: A state of the art," *Progress in Energy and Combustion Science*, vol. 93, p. 101026, 2022/11/01/ 2022. https://doi.org/10.1016/j.pecs.2022.101026

[16] K. Zhang and H. C. Lau, "Sequestering CO2 as CO2 hydrate in an offshore saline aquifer by reservoir pressure management," *Energy*, vol. 239, p. 122231, 2022/01/15/ 2022. https://doi.org/10.1016/j.energy.2021.122231

[17] L. Jiao, R. Wan, and Z. Wang, "Experimental investigation of CO2 hydrate formation in silica nanoparticle system under static conditions," *Journal of Crystal Growth*, vol. 583, p. 126539, 2022/04/01/ 2022. https://doi.org/10.1016/j.jcrysgro.2022.126539

[18] F. Wang *et al.*, "Dynamic mechanism of CO2 capture from flue gas via hydrate-based method induced by using IB group transition metal functionalized carbon nanotubes," *Gas Science and Engineering*, vol. 128, p. 205392, 2024/08/01/ 2024. https://doi.org/10.1016/j.jgsce.2024.205392

[19] S. Jia *et al.*, "Rapid growth of CO2 hydrate as a promising way to mitigate the greenhouse effect," *Materials Today Physics*, vol. 48, p. 101548, 2024/11/01/ 2024. https://doi.org/10.1016/j.mtphys.2024.101548

[20] S. Ma *et al.*, "Formation and decomposition characteristics of CO2+TBAB hydrate for a safer CO2 storage," *Energy*, vol. 307, p. 132801, 2024/10/30/ 2024. https://doi.org/10.1016/j.energy.2024.132801

[21] A. Kumar, T. Sakpal, P. Linga, and R. Kumar, "Influence of contact medium and surfactants on carbon dioxide clathrate hydrate kinetics," *Fuel*, vol. 105, pp. 664-671, 2013/03/01/ 2013. https://doi.org/10.1016/j.fuel.2012.10.031

[22] Y.-s. Yu, C.-g. Xu, and X.-s. Li, "Evaluation of CO2 hydrate formation from mixture of graphite nanoparticle and sodium dodecyl benzene sulfonate," *Journal of Industrial and Engineering Chemistry*, vol. 59, pp. 64-69, 2018/03/25/ 2018. https://doi.org/10.1016/j.jiec.2017.10.007

[23] X. Zang, L. Wan, Y. He, and D. Liang, "CO2 removal from synthesized ternary gas mixtures used hydrate formation with sodium dodecyl sulfate(SDS) as additive," *Energy*, vol. 190, p. 116399, 2020/01/01/ 2020. https://doi.org/10.1016/j.energy.2019.116399

[24] X. Liu, J. Ren, D. Chen, and Z. Yin, "Comparison of SDS and L-Methionine in promoting CO2 hydrate kinetics: Implication for hydrate-based CO2 storage," *Chemical Engineering Journal*, vol. 438, p. 135504, 2022/06/15/ 2022. https://doi.org/10.1016/j.cej.2022.135504

[25] S. Al-Anssari, A. Barifcani, S. Wang, M. Lebedev, and S. Iglauer, "Wettability alteration of oil-wet carbonate by silica nanofluid," *Journal of Colloid and Interface Science*, vol. 461, pp. 435-442, 1/1/ 2016. http://dx.doi.org/10.1016/j.jcis.2015.09.051

[26] M. Mahdi, S. Al-Anssari, and Z.-U.-A. Arain, "Influence of nanofluid flooding on oil displacement in porous media," *Iraqi Journal of Chemical and Petroleum Engineering*, vol. 24, no. 2, pp. 19-30, 2023. https://doi.org/10.31699/IJCPE.2023.2.3

[27] S. Al-Anssari, M. Arif, S. Wang, A. Barifcani, M. Lebedev, and S. Iglauer, "CO2 geo-storage capacity enhancement via nanofluid priming," *International Journal of Greenhouse Gas Control*, vol. 63, pp. 20-25, 2017. https://doi.org/10.1016/j.ijggc.2017.04.015

[28] S.-D. Zhou *et al.*, "The synergistic promotion of L-methionine combined with multi-walled carbon nanotubes on CO2 hydrate formation kinetics," *Journal of Industrial and Engineering Chemistry*, vol. 138, pp. 282-299, 2024/10/25/ 2024. https://doi.org/10.1016/j.jiec.2024.04.004

[29] S. Chol, "Enhancing thermal conductivity of fluids with nanoparticles," *ASME-Publications-Fed*, vol. 231, pp. 99-106, 1995.

[30] J. Li, D. Liang, K. Guo, R. Wang, and S. Fan, "Formation and dissociation of HFC134a gas hydrate in nano-copper suspension," *Energy Conversion and Management*, vol. 47, no. 2, pp. 201-210, 2006/01/01/ 2006. https://doi.org/10.1016/j.enconman.2005.03.018

[31] V. D. Chari, D. V. S. G. K. Sharma, P. S. R. Prasad, and S. R. Murthy, "Methane hydrates formation and dissociation in nano silica suspension," *Journal of Natural Gas Science and Engineering*, vol. 11, pp. 7-11, 2013/03/01/ 2013. https://doi.org/10.1016/j.jngse.2012.11.004

[32] M. Mohammadi, A. Haghtalab, and Z. Fakhroueian, "Experimental study and thermodynamic modeling of CO2 gas hydrate formation in presence of zinc oxide nanoparticles," *The Journal of Chemical Thermodynamics*, vol. 96, pp. 24-33, 2016/05/01/ 2016. https://doi.org/10.1016/j.jct.2015.12.015

[33] Y.-s. Yu, S.-d. Zhou, X.-s. Li, and S.-l. Wang, "Effect of graphite nanoparticles on CO2 hydrate phase equilibrium," *Fluid Phase Equilibria*, vol. 414, pp. 23-28, 2016/04/25/ 2016. https://doi.org/10.1016/j.fluid.2015.12.054

[34] Z. Cheng *et al.*, "Effect of nanoparticles as a substitute for kinetic additives on the hydrate-based CO2 capture," *Chemical Engineering Journal*, vol. 424, p. 130329, 2021/11/15/ 2021. https://doi.org/10.1016/j.cej.2021.130329

[35] S. Kim, A. H. Zadeh, M. Nole, H. Daigle, C. Huh, and I. Kim, "Spontaneous generation of stable CO2 emulsions via the dissociation of nanoparticle-aided CO2 hydrate," *Journal of Petroleum Science and Engineering*, vol. 208, p. 109203, 2022/01/01/ 2022. https://doi.org/10.1016/j.petrol.2021.109203

[36] A. Mohammadi, M. Manteghian, A. Haghtalab, A. H. Mohammadi, and M. Rahmati-Abkenar, "Kinetic study of carbon dioxide hydrate formation in presence of silver nanoparticles and SDS," *Chemical Engineering Journal*, vol. 237, pp. 387-395, 2014/02/01/ 2014. https://doi.org/10.1016/j.cej.2013.09.026

[37] H. Pahlavanzadeh, M. Khanlarkhani, S. Rezaei, and A. H. Mohammadi, "Experimental and modelling studies on the effects of nanofluids (SiO2, Al2O3, and CuO) and surfactants (SDS and CTAB) on CH4 and CO2 clathrate hydrates formation," *Fuel*, vol. 253, pp. 1392-1405, 2019/10/01/ 2019. https://doi.org/10.1016/j.fuel.2019.05.010

[38] S. Rajabi Firoozabadi and M. Bonyadi, "A comparative study on the effects of Fe3O4 nanofluid, SDS and CTAB aqueous solutions on the CO2 hydrate formation," *Journal of Molecular Liquids*, vol. 300, p. 112251, 2020/02/15/ 2020. https://doi.org/10.1016/j.molliq.2019.112251

[39] D. Bai, G. Chen, X. Zhang, A. K. Sum, and W. Wang, "How properties of solid surfaces modulate the nucleation of gas hydrate," *Scientific reports*, vol. 5, no. 1, p. 12747, 2015. https://doi.org/10.1038/srep12747

[40] N. N. Nguyen, A. V. Nguyen, K. M. Steel, L. X. Dang, and M. Galib, "Interfacial Gas Enrichment at Hydrophobic Surfaces and the Origin of Promotion of Gas Hydrate Formation by Hydrophobic Solid Particles," *The Journal of Physical Chemistry C*, vol. 121, no. 7, pp. 3830-3840, 2017/02/23 2017. https://doi.org/10.1021/acs.jpcc.6b07136

[41] I. Kim *et al.*, "Highly porous CO2 hydrate generation aided by silica nanoparticles for potential secure storage of CO2 and desalination," *RSC Advances*, 10.1039/C6RA26366F vol. 7, no. 16, pp. 9545-9550, 2017. https://doi.org/10.1039/C6RA26366F

[42] R. Wang *et al.*, "Effect of hydrophilic silica nanoparticles on hydrate formation: Insight from the experimental study," *Journal of Energy Chemistry*, vol. 30, pp. 90-100, 2019/03/01/ 2019. https://doi.org/10.1016/j.jechem.2018.02.021

[43] J. Min, D. W. Kang, W. Lee, and J. W. Lee, "Molecular Dynamics Simulations of Hydrophobic Nanoparticle Effects on Gas Hydrate Formation," *The Journal of Physical Chemistry C*, vol. 124, no. 7, pp. 4162-4171, 2020/02/20 2020. https://doi.org/10.1021/acs.jpcc.9b11459

[44] Z.-U. L. A. Arain *et al.*, "Reversible and irreversible adsorption of bare and hybrid silica nanoparticles onto carbonate surface at reservoir condition," *Petroleum*, vol. 6, no. 3, pp. 277-285, 2020/09/01/ 2020. https://doi.org/10.1016/j.petlm.2019.09.001

[45] J. W. Grate *et al.*, "Correlation of Oil–Water and Air–Water Contact Angles of Diverse Silanized Surfaces and Relationship to Fluid Interfacial Tensions," *Langmuir*, vol. 28, no. 18, pp. 7182-7188, 2012/05/08 2012. https://doi.org/10.1021/la204322k

[46] W. He *et al.*, "Surface modification of colloidal silica nanoparticles: Controlling the size and grafting process," *Bulletin of the Korean Chemical Society*, vol. 34, no. 9, pp. 2747-2752, 2013. https://doi.org/10.5012/bkcs.2013.34.9.2747

[47] G. London, G. T. Carroll, and B. L. Feringa, "Silanization of quartz, silicon and mica surfaces with light-driven molecular motors: construction of surface-bound photo-active nanolayers," *Organic & Biomolecular Chemistry*, 10.1039/C3OB40276B vol. 11, no. 21, pp. 3477-3483, 2013. https://doi.org/10.1039/C3OB40276B

[48] P. Rostamzadeh, S. M. Mirabedini, and M. Esfandeh, "APS-silane modification of silica nanoparticles: effect of treatment's variables on the grafting content and colloidal stability of the nanoparticles," *Journal of Coatings Technology and Research*, journal article vol. 11, no. 4, pp. 651-660, 2014. https://doi.org/10.1007/s11998-014-9577-8

[49] S. Al-Anssari, M. Arif, S. Wang, A. Barifcani, and S. Iglauer, "Stabilising nanofluids in saline environments," *Journal of Colloid and Interface Science*, vol. 508, pp. 222-229, 2017. https://doi.org/10.1016/j.jcis.2017.08.043

[50] N. Bajpai, A. Tiwari, S. Khan, R. Kher, N. Bramhe, and S. Dhoble, "Effects of rare earth ions (Tb, Ce, Eu, Dy) on the thermoluminescence characteristics of sol–gel derived and γ-irradiated SiO2 nanoparticles," *Luminescence*, vol. 29, no. 6, pp. 669-673, 2014. https://doi.org/10.1002/bio.2604

[51] S. Al-Anssari *et al.*, "Synergistic effect of nanoparticles and polymers on the rheological properties of injection fluids: implications for enhanced oil recovery," *Energy & Fuels*, vol. 35, no. 7, pp. 6125-6135, 2021. https://doi.org/10.1021/acs.energyfuels.1c00105

[52] S. Al-Anssari, A. Barifcani, A. Keshavarz, and S. Iglauer, "Impact of nanoparticles on the CO2-brine interfacial tension at high pressure and temperature," *Journal of Colloid and Interface Science*, vol. 532, pp. 136-142, 2018/12/15/ 2018. https://doi.org/10.1016/j.jcis.2018.07.115

[53] S. Al-Anssari, H. A. Shanshool, A. Keshavarz, and M. Sarmadivaleh, "Synergistic effect of hydrophilic nanoparticles and anionic surfactant on the stability and viscoelastic properties of oil in water (o/w) emulations; application for enhanced oil recovery (EOR)," *Journal of Petroleum Research and Studies*, vol. 10, no. 4, pp. 33-53, 2020. https://doi.org/10.52716/jprs.v10i4.366

[54] S. Al-Anssari, Z.-U. L. A. Arain, A. Barifcani, A. Keshavarz, M. Ali, and S. Iglauer, "Influence of Pressure and Temperature on CO2-Nanofluid Interfacial Tension: Implication for Enhanced Oil Recovery and Carbon Geosequestration," presented at the Abu Dhabi International Petroleum Exhibition & Conference, Abu Dhabi, UAE, 2018/11/12/, 2018. https://doi.org/10.2118/192964-MS

تعزيز تكون هيدرات ثاني أكسيد الكربون (اتحاد الغاز بالماء) باستخدام جزيئات السيليكا المجردة والهجينة: تأثيرها وتطبيقاتها في عزل ثاني أكسيد الكربون القائم على الهيدرات

سرمد الأنصاري [١، ٢، ٣، *]، ضفاف صادق [٢، ٤]، حسنين عباس حسن [١]،
أحمد حامد الطائي [٤، ٥]، زين العابدين عريان [٦]

١ قسم الهندسة الكيميائية، كلية الهندسة، جامعة بغداد، بغداد، العراق
٢ قسم هندسة النفط، كلية الهندسة، جامعة الناجي، بغداد، العراق
٣ كلية الهندسة، جامعة إديث كوان، جوندالوب، أستراليا
٤ قسم هندسة النفط، كلية الهندسة، جامعة بغداد، بغداد، العراق
٥ جامعة غوبكين الروسية الحكومية للنفط والغاز، موسكو، روسيا
٦ كلية أستراليا الغربية للمناجم والمعادن والطاقة والهندسة الكيميائية، جامعة كيرتن، ٢٦ شارع ديك بيري، كنسينغتون ٦١٥١، WA، أستراليا

الخلاصة

يُقدم التخزين الجيولوجي لثاني أكسيد الكربون امكانيات هائلة للتخفيف من انبعاثات الكربون الناتجة من الانشطة البشرية. وقد حظيت هيدرات ثاني أكسيد الكربون باهتمام متزايد نظرًا لإمكاناتها في مشاريع عزل الكربون الجيولوجي. اجريت دراسة منهجية لتأثير جسيمات السيليكا النانوية (SiNPs) على حركية تكوين هيدرات ثاني أكسيد الكربون عند ضغط ٣,٥ MPa ودرجة حرارة ٢٨٠ K. تم وُصفت جسيمات السيليكا النانوية النقية (المجردة) والمعدلة سطحيًا (الهجينة)، واستُخدمت في هذه الدراسة بشكل منفصل. تم دراسة آثار تركيز جسيمات السيليكا النانوية المجردة والهجينة على زمن تفعيل تكوين هيدرات ثاني أكسيد الكربون. استُخدم مفاعل من الفولاذ المقاوم للصدأ عالي الضغط وعالي الحرارة كمفاعل هيدرات، وسُجلت بيانات الضغط ودرجة الحرارة باستمرار لمتابعة عملية تكوين الهيدرات. كشفت النتائج أن جسيمات السيليكا النانوية تؤثر بشكل كبير على حركية تكوين هيدرات ثاني أكسيد الكربون. إن زيادة تركيز جسيمات النانو النانوية السيليكونية الهجينة (<٠,٠٣% وزناً) تُقلل بشكل ملحوظ من زمن التفعيل، وبالتالي تُسرّع من سرعة تكوين هيدرات ثاني أكسيد الكربون. في المقابل، أظهرت جسيمات النانو النانوية السيليكونية المجردة تأثيراً أقل على تكوين هيدرات ثاني أكسيد الكربون. علاوة على ذلك، فإن زيادة تركيز جسيمات النانو النانوية السيليكونية المجردة (مثلاً،<٠,٠٧% وزناً) قد تُقلل من تأثير جسيمات النانو النانوية على زمن التفعيل. وبالتالي، يُمكن لجسيمات النانو النانوية السيليكونية المُعدّلة سطحياً أن تُعزز بشكل كبير تكوين هيدرات ثاني أكسيد الكربون عند صياغتها بشكل صحيح.

الكلمات الدالة: هيدرات ثاني أكسيد الكربون، تخزين الكربون، جسيمات السيليكا النانوية، السوائل النانوية، حركية التكوين.